



<b>Title</b>	<b>A reconfigurable wideband and multiband antenna using dual-patch elements for compact wireless devices</b>
<b>Author(s)</b>	<b>Abutarboush, HF; Nilavalan, R; Cheung, SW; Nasr, KM; Peter, T; Budimir, D; Al-Raweshidy, H</b>
<b>Citation</b>	<b>IEEE Transactions On Antennas And Propagation, 2012, v. 60 n. 1, p. 36-43</b>
<b>Issued Date</b>	<b>2012</b>
<b>URL</b>	<b><a href="http://hdl.handle.net/10722/155722">http://hdl.handle.net/10722/155722</a></b>
<b>Rights</b>	<b>IEEE Transactions on Antennas and Propagation. Copyright © IEEE.</b>

# A Reconfigurable Wideband and Multiband Antenna Using Dual-Patch Elements for Compact Wireless Devices

Hattan F. Abutarboush, *Member, IEEE*, R. Nilavalan, *Senior Member, IEEE*, S. W. Cheung, *Senior Member, IEEE*, Karim M. Nasr, *Senior Member, IEEE*, Thomas Peter, *Djuradj Budimir, Senior Member, IEEE*, and Hamed Al-Raweshidy, *Senior Member, IEEE*

**Abstract**—A reconfigurable wideband and multiband C-Slot patch antenna with dual-patch elements is proposed and studied. It occupies a compact volume of  $50 \times 50 \times 1.57$  (3925 mm<sup>3</sup>), including the ground plane. The antenna can operate in two dual-band modes and a wideband mode from 5 to 7 GHz. Two parallel C-Slots on the patch elements are employed to perturb the surface current paths for excitation of the dual-band and the wideband modes. Two switches, implemented using PIN diodes, are placed on the connecting lines of a simple feed network to the patch elements. Dual-band modes are achieved by switching “ON” either one of the two patch elements, while the wideband mode with an impedance bandwidth of 33.52% is obtained by switching “ON” both patch elements. The frequencies in the dual-band modes can be independently controlled using positions and dimensions of the C-Slots without affecting the wideband mode. The advantage of the proposed antenna is that two dual-band operations and one wideband operation can be achieved using the same dimensions. This overcomes the need for increasing the surface area normally incurred when designing wideband patch antennas. Simulation results are validated experimentally through prototypes. The measured radiation patterns and peak gains show stable responses and are in good agreements. Coupling between the two patch elements plays a major role for achieving the wide bandwidth and the effects of mutual coupling between the patch elements are also studied.

**Index Terms**—C-slot, cognitive radio, patch antenna, reconfigurable antenna, slot antenna, small antenna, switched antenna, wideband antenna.

## I. INTRODUCTION

PATCH antennas suffer from narrow bandwidth which can limit their uses in some modern wireless applications [1], [2]; therefore, there is an increasing demand for low-profile,

easy to manufacture, and multiband/wideband antennas which can be easily integrated within communication systems. A variety of studies have come up with different techniques to achieve wideband operation for printed antennas. Some of the techniques employed are changing the physical size of the antenna, modifying the radiator shape to allow current paths to travel at longer distances (which sometime increases the antenna size), and adding additional parts such as multi layers or gaps (which again makes the antenna larger and of a higher profile). Other techniques include using U-slot array [3], shorting wall [4], folded shorting wall [5], Y-V Slot [6], slots form [7], stacked patch [8], pair of slits on the patch (with total size of the antenna  $150 \times 150 \times 14.3$  mm<sup>2</sup>) [9], E-shaped patch on thick substrates with ground plane size of  $140 \times 210$  mm<sup>2</sup> [10] and using circular arc shaped slot on thick substrate [11]. The designs in [3]–[11] can achieve wide impedance bandwidths. However, these antennas are large in sizes and difficult to fit into small and slim devices.

A reconfigurable antenna is another solution to achieve a wide impedance bandwidth by switching ON and OFF some parts of the antenna. To allow the operating frequencies and the bandwidths to be reconfigurable, switching components are normally used. PIN diodes, varactor diodes or MEMS switches are the most frequently used components in the design of reconfigurable antennas [12]–[15]. In literature, few papers reported the approach of switching between wideband and narrowband operations. For example in [16]–[18], studies were done on switching between dual ports, one port for Ultra Wideband (UWB) and the other port for a single narrowband. However, the use of an UWB antenna for multiband applications could result in unwanted emissions in the transmission mode.

In this paper, a single-feed reconfigurable wideband and multiband antenna using two patch elements on a planar structure is proposed. Two C-Slots are employed on the patch elements for excitation of the dual-band and wideband modes. Two PIN diode switches are placed on the connecting lines of a simple feed network to the patch elements. Dual-band and wideband-mode operations are obtained by switching “ON/OFF” the two patch elements. The antenna can be used for narrowband applications such as the WLAN and WiMAX and wideband operations in the frequency range from 5 to 7 GHz for other wireless standards. The design eliminates the need for using two ports as proposed in [17], [18] and increases the number of possible frequency bands from one to four. The

Manuscript received January 10, 2011; revised April 15, 2011; accepted July 12, 2011. Date of publication September 15, 2011; date of current version January 05, 2012. The measurements at the NPL SMART chamber were supported by the Measurements for Innovators (MFI) program and the National Measurement Office, an Executive Agency of the Department for Business, Innovation and Skills.

H. F. Abutarboush, R. Nilavalan, T. Peter, and H. Al-Raweshidy are with the Wireless Networks and Communications Centre (WNCC), School of Engineering and Design, Brunel University, West London UB8 3PH, U.K. (e-mail: hattan.abutarboush@ieee.org).

S. W. Cheung is with the Department of Electrical and Electronics Engineering, Hong Kong University, Hong Kong, China.

K. M. Nasr is with the National Physical Laboratory (NPL), Teddington TW11 0LW, U.K.

D. Budimir is with the Wireless Communications Research Group, Department of Electronics and Computer Science, Westminster University, London W1W 6UW, U.K.

Color versions of one or more of the figures in this paper are available online at <http://ieeexplore.ieee.org>.

Digital Object Identifier 10.1109/TAP.2011.2167925

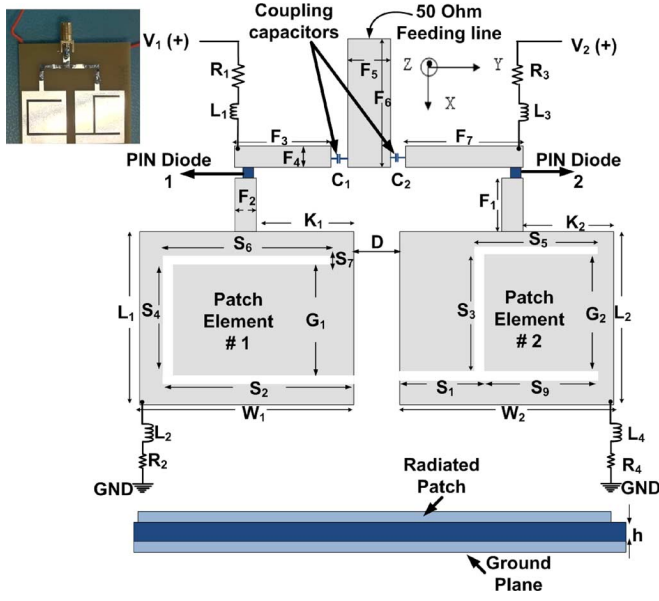


Fig. 1. Configuration of proposed antenna with dc biasing networks.

TABLE I  
DETAILED DIMENSIONS OF PROPOSED ANTENNA (UNITS IN mm)

$L_1$	$W_1$	$L_2$	$W_2$	$S_1$	$S_2$	$S_3$	$S_4$	$S_5$
24	20	24	22	9	18	14	14	12
$S_6$	$S_7$	$S_8$	$F_1$	$F_2$	$F_3$	$F_4$	$F_5$	$F_6$
16	1	11	9	2	9	2	3	11.6
$F_7$	$D$	$K_1$	$K_2$	$G_1$	$G_2$	$h$	Ground Plane Area	
12	4	9	11	14	16	1.57	50 x 50	

volume of the proposed antenna, including the ground plane and the substrate, is 50 mm × 50 mm × 1.57 mm. The design can also be used for cognitive radio applications as described in [19].

## II. ANTENNA CONFIGURATION AND DESIGN PROCEDURE

Fig. 1 shows the schematic diagram of our proposed reconfigurable antenna which consists of two patch elements (patch elements #1 and #2) with a simple feed network, two PIN-diode switches and two chip capacitors all on one side of the substrate and a ground plane on the other side of the substrate. The complete antenna is designed using the EM simulator, HFSS V.11.2, based on finite elements modeling (FEM) and fabricated on an FR-4 substrate with thickness of 1.57 mm and a relative permittivity of  $\epsilon_r = 4.4$ . The key antenna parameters of the antenna are shown in Table I.

The dimensions of the patch elements of the antenna are optimized to operate in the 5.5-GHz WLAN band. Since cutting a slot on the radiator can change the current distribution and the current path, and hence improve the impedance matching especially at higher frequencies, as discussed in [20] and [21], in our design, we use two C-Slots on the two patch elements, as shown in Fig. 1, to generate a wide impedance bandwidth and to create multiple resonant frequencies. The feed network has a main 50- $\Omega$  feed line and two connecting lines which have been optimized, in terms of impedance bandwidth, to have a

line impedance of 63  $\Omega$ . Two PIN diodes are placed on the connecting lines to the patch elements and used as switches. Just to prove our design concept, we have used the practical PIN diodes, SMP1320-079 from Skyworks Solutions Inc. with a size of  $1.5 \times 0.7 \text{ mm}^2$ , as the switches. In computer simulation, these two diodes are modeled using the resistance, inductance, and capacitance (RLC) boundary sheet which gives 0.9  $\Omega$  as the impedance value of the PIN diode in the ON state and 0.3 pF as the capacitance value in the OFF state. These PIN diodes are turned “ON/OFF” using a dc biased signal, so two coupling chip capacitors ( $C_1$  and  $C_2$ ) each with 10 pF are used to prevent the dc signal from flowing to the main feed line but allow the RF current to pass through. The biasing networks for the two PIN diodes are also shown in Fig. 1, where the inductors  $L_1$ ,  $L_2$ ,  $L_3$  and  $L_4$ , all with 12 nH, are used as radio-frequency (RF) chokes to provide high impedance for the RF signals. The resistors,  $R_1$ ,  $R_2$ ,  $R_3$  and  $R_4$ , each with 10 k $\Omega$ , are used to control the dc biasing current to (or dc biasing voltage of about 0.7 V across) the PIN diodes. These lumped components will have insignificant effects on the antenna performance because the impedances of the RL circuits are much higher than the impedance of the antenna, allowing very little currents to flow through.

## III. SIMULATION AND MEASUREMENTS RESULTS

### A. Impedance Bandwidth for $S_{11} < -10 \text{ dB}$

The two PIN diodes provide three possible and useful switching states, i.e., ON-OFF, OFF-ON, and ON-ON states (note that the OFF-OFF state has no practical use). Simulation tests using the HFSS have been carried out on the impedance bandwidth (for reflection coefficient  $S_{11} < -10 \text{ dB}$ ) of the antenna in different states. In the OFF-ON state, only patch element #2 is ON and functioning. Simulation results in Fig. 2(a) show that a dual-band is obtained at 5.6 and 6.2 GHz, with the respective bandwidths of 5.2% and 4.85%. In the ON-OFF state, only patch element #1 of the antenna is ON and radiating. The results in Fig. 2(b) show that another dual-band mode is obtained at 5 and 5.7 GHz, with the corresponding impedance bandwidth of 4.2% and 2.4%. In the ON-ON state, both patch elements are radiating. A wide bandwidth of 33.52%, covering the frequency range from 4.99 to 7 GHz, is obtained as shown in Fig. 2(c). To validate the simulation results, the proposed antenna has also been fabricated and the  $S_{11}$  in the ON-OFF, OFF-ON, and ON-ON states have been measured using Agilent N5230A vector network analyzer. Results are shown in Fig. 2(a)–(c) for comparison. It can be seen that the simulated and measured results are in good agreements. The small discrepancies between the simulated and measured results could be attributed to the fabrication accuracy of the prototype.

### B. Effects of C-Slots

Multiband operation of the antenna is achieved mainly by the C-Slots on the patch elements. Simulation tests have been carried out to study the  $S_{11}$  of the antenna without the C-Slots in the ON-OFF and OFF-ON states. Fig. 3 compares the  $S_{11}$  with and without the C-Slots in the patch elements. In the ON-OFF state when patch element #1 is active and patch element #2 is OFF,

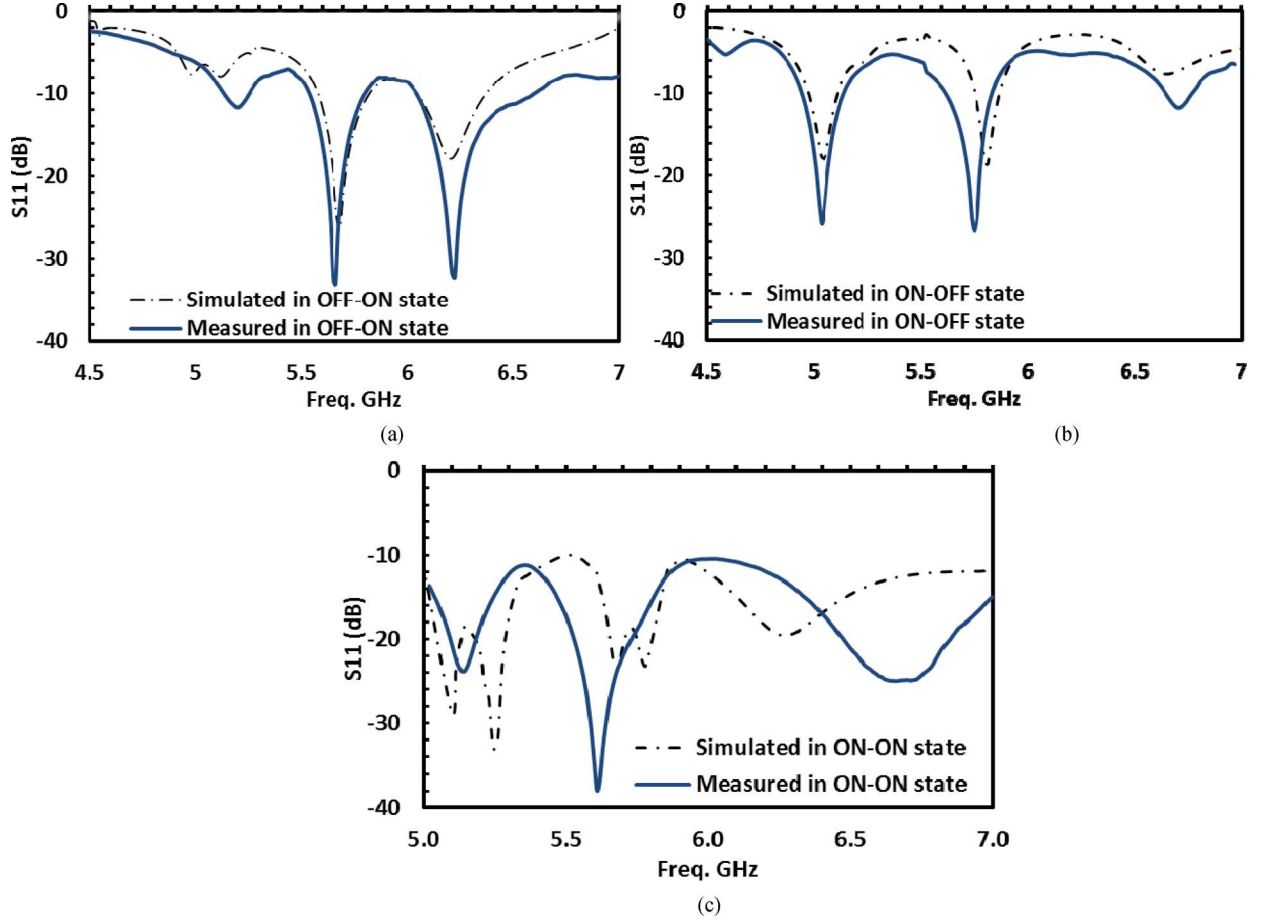


Fig. 2. Simulated and measured  $S_{11}$  of proposed antenna in (a) OFF-ON, (b) ON-OFF, and (c) ON-ON states.

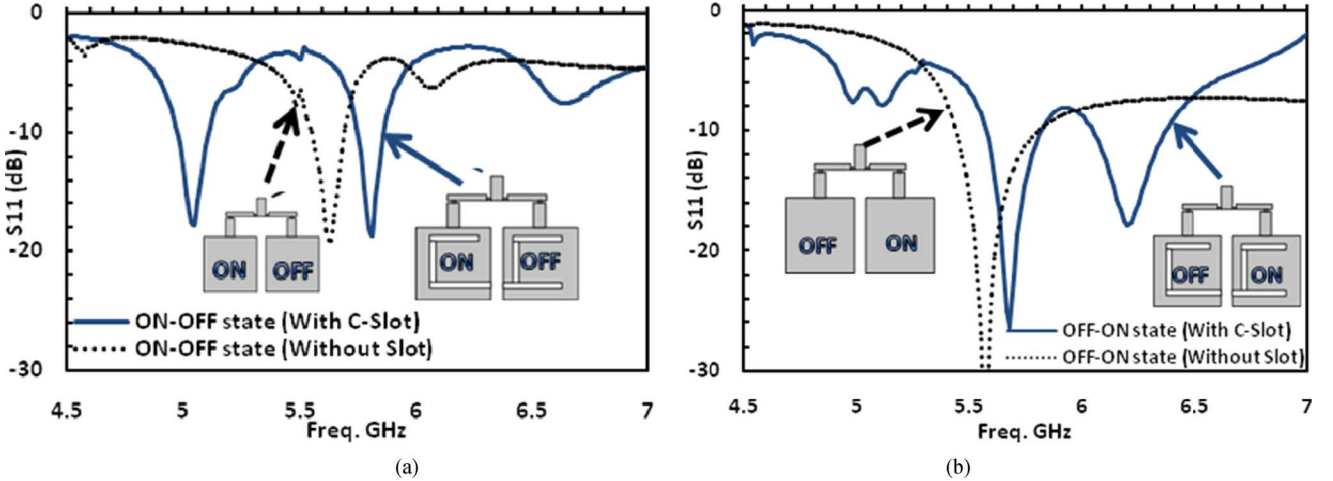


Fig. 3. Effects of C-Slots on  $S_{11}$  in (a) ON-OFF and (b) OFF-ON states.

Fig. 3(a) shows that, without the C-Slots, the antenna has a resonant frequency at 5.6 GHz. While with the C-Slots, a dual-band is generated at 5 and 5.7 GHz. In the OFF-ON state when patch element #2 is turned ON and patch element #2 is OFF, Fig. 3(b) shows that the antenna without the C-Slots has a single band at 5.55 GHz. While with the C-Slots on the patch elements, a dual-band is generated at 5.6 and 6.2 GHz. Therefore, the C-Slots on the patch elements help generate a dual band. Moreover, simulation results have also shown that the widths and the lengths of the patch elements determine the centre frequencies

in the single-band cases. While the positions and dimensions of the C-Slots on the patch elements determine the centre frequencies in the dual-band cases. The simulated-frequency bands generated with and without the C-Slots in our design are summarized in Table II.

### C. Current Distributions

Cutting slots on the radiator of an antenna can change the current path and so can be used to generate dual-band or even multiple-bands operations. In our proposed design, if the slots



TABLE II  
GENERATED BANDS WITH AND WITHOUT C-SLOTS

State	Without Slots	With C-Slots
OFF ON	5.55 GHz	5.6 & 6.2 GHz
ON OFF	5.6 GHz	5 & 5.7 GHz
ON ON	5.55 & 5.65 GHz	Wideband from 5 to 7 GHz

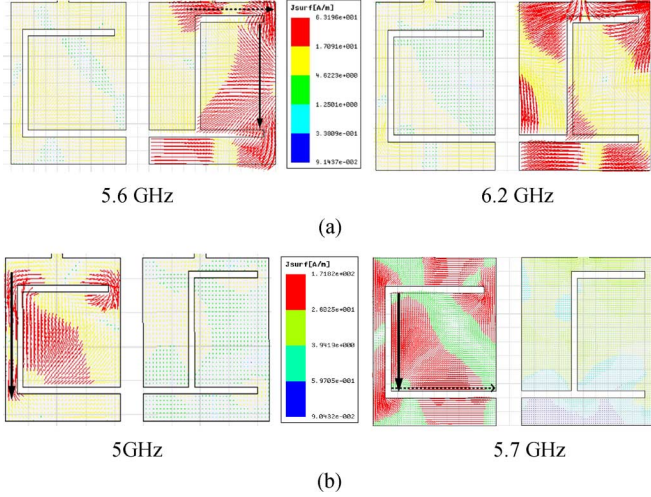


Fig. 4. Simulated current distributions in (a) OFF-ON and (b) ON-OFF states.

are absent, the antenna will have only one major current path on each of the patch elements. However, in the presence of the two C-slots, the current path on each of the patch elements is disturbed, hence creating the dual-band operation. Fig. 4 shows the simulated current distributions on the patch elements in different switching states. In the OFF-ON state, patch element #2 is radiating and patch element #1 is OFF. Fig. 4(a) shows that the current travels around the C-Slot on patch element #2, as expected, generating the resonant frequencies at 5.6 and 6.2 GHz as shown in Fig. 2(a) for the WLAN 802.11a/h/j/n applications. In the ON-OFF state, only patch element #1 is ON and radiating and patch element #2 is OFF. Fig. 4(b) shows that the current travels around the C-Slot on patch element #1, generating the dual band at 5 and 5.7 GHz as shown in Fig. 2(b), for the WLAN 802.11a/h/j/n applications. The dominate current paths for OFF-ON and ON-OFF states are shown in Fig. 4. These paths correspond to approximately  $0.5\lambda$ , where  $\lambda$  is the wavelength at the resonant frequency of the respective band and given by  $\lambda = \lambda_0 / \sqrt{(\epsilon_r + 1)/2}$ , with  $\lambda_0$  being the free space wavelength. The 6.2-GHz band in the OFF-ON case is generated from a higher order mode. In the ON-ON state where both patch elements are ON, the wideband operation is obtained by coupling which will be explained later.

#### D. Measured Radiation Patterns and Gains

The radiation patterns of the antenna have been measured using the Small Antenna Radiated Testing Range (SMART) at the National Physical Laboratory (NPL), with results normalized to the maximum values. Figs. 6–8 show the measured and simulated co- and cross-polarization patterns of the antenna in different switch states at several frequencies across the operating bandwidth.

In the OFF-ON and ON-OFF states, the radiation patterns at the pair-resonant frequencies of 5.6 and 6.2 GHz, and 5 and 5.7 GHz, respectively, are used for comparison. In the ON-ON state where the antenna has an operation bandwidth from 5 to 7 GHz, the radiation patterns at the extreme frequencies of 5 and 7 GHz and the middle frequency of 6 GHz are studied. From the current distributions shown in Fig. 4, it can be seen that the directions of the dominant currents at the frequencies studied are mainly in the X-direction, so the Y-Z and X-Z planes are the H- and E-planes, respectively. As a result, the co-polarization patterns in Figs. 5–7 are all relatively unidirectional toward the Z-direction with small back radiation due to the finite ground-plane size. The high cross polarizations at 5.6 and 5.7 GHz in the OFF-ON and ON-OFF states are due to high current concentration in the Y-Directions. Some minor discrepancies occur between the simulated and measured results, which could be due to the effect of the coaxial cable connected to the antenna during measurements.

The peak gains of the antenna at different frequencies are between 3 and 5 dBi in different switching states and summarized in Table III. The simulated radiation efficiency of the antenna in the ON-ON state ranges from 60% to 70%.

#### IV. INDEPENDENT CONTROL OF EACH BANDS

To design antennas with multiple-band operations, it is desirable to have independent-frequency controls on the frequencies. Achieving this option is very challenging. Very often, when one parameter is changed, all the frequency bands are affected [22], [23] and the antenna needs to be completely re-optimized. Sometimes, the shape of the designed antenna has to be significantly changed, causing a lot of inconvenience in designing wireless devices.

Results in previous sections have shown that, in the ON-OFF and OFF-ON states, the C-Slots on the patch elements of the antenna can be used to generate two frequency bands for dual-band operation. Here, we show how to use the C-Slots to independently control the frequency bands for dual-band operation without affecting the wideband operation. In the ON-OFF state, the simulation results in Fig. 8(a) shows the effects of changing the length  $S_4$  in the slot of patch element #1 on the lower band of the dual band. It can be seen that increasing  $S_4$  moves the 5-GHz band lower but keeps the 5.7-GHz band fixed (Note,  $G_1$  is kept fixed here). Fig. 8(b) shows that the effect of changing  $W_1$  and  $S_2$  together on the higher band of the dual band. Here, reducing  $W_1$  and  $S_2$  together moves the 5.7-GHz band to a higher frequency band, yet the 5-GHz band remains unchanged. In the OFF-ON state, Fig. 9(a) shows the effects of changing the size of  $S_5$ , indicating that the length of  $S_5$  can be used to move the lower band (at around 5.6 GHz), yet keeping the 6.2-GHz band fixed. Finally, Fig. 9(b) shows that changing the distance  $G_2$  (i.e., moving  $S_1$  and  $S_9$  together closer or further from  $S_5$  while keeping  $S_3$  the same) can shift the higher band (at around 6.2 GHz) to a higher or lower frequency band, yet maintaining the 5.6-GHz band. It should be noted that, in some cases, after fixing the frequency of the band, we may need to optimize the other parameters of the antenna to achieve the desirable  $S_{11}$ . These results show that we can independently control the frequencies of the dual bands by using the C-Slots on

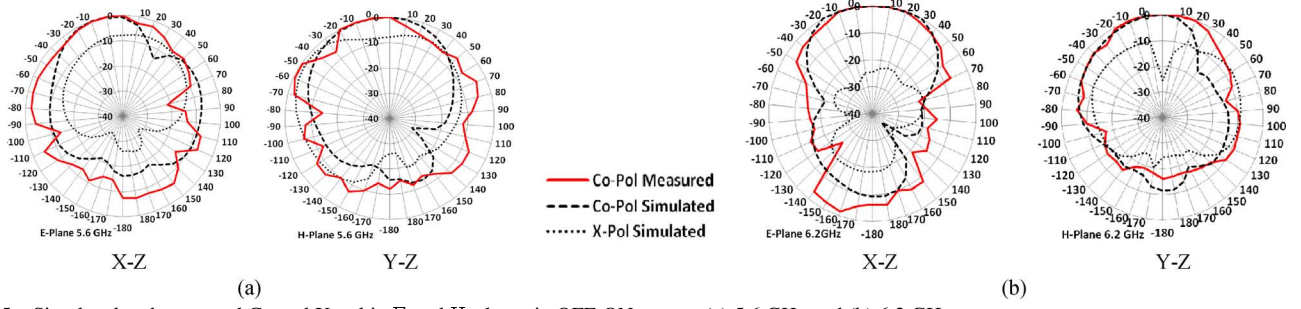


Fig. 5. Simulated and measured Co and X-pol in E and H-planes in OFF-ON state at (a) 5.6 GHz and (b) 6.2 GHz.

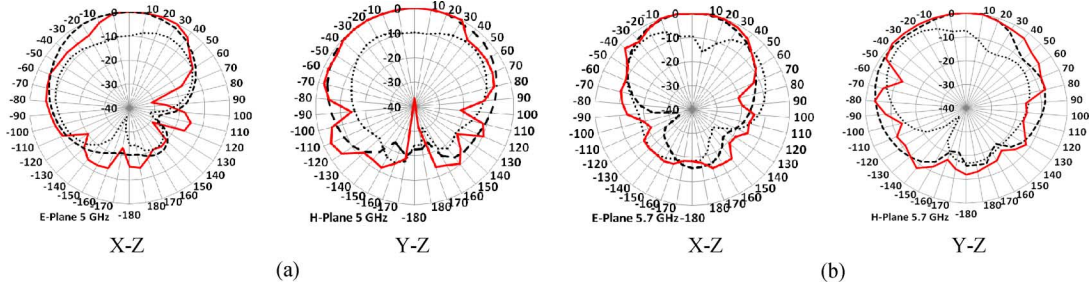


Fig. 6. Simulated and measured Co and X-pol in E and H-planes in ON-OFF state at (a) 5 GHz and (b) 5.7 GHz.

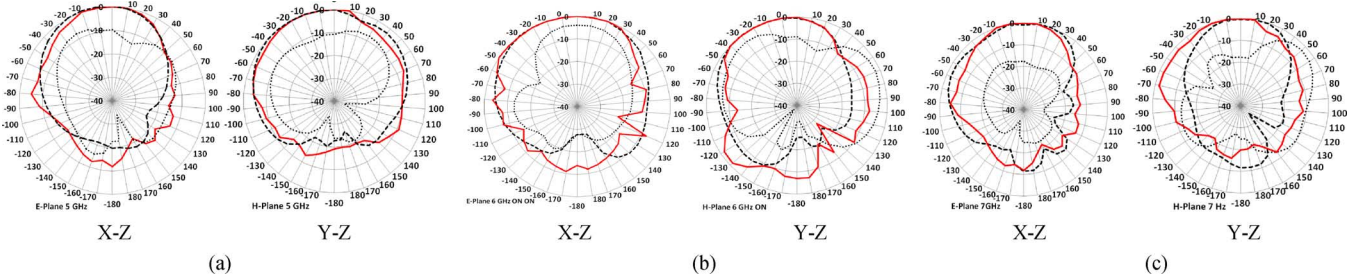


Fig. 7. Simulated and measured Co and X-pol in E and H-planes in ON-ON state at (a) 5 GHz, (b) 6 GHz, and (c) 7 GHz.

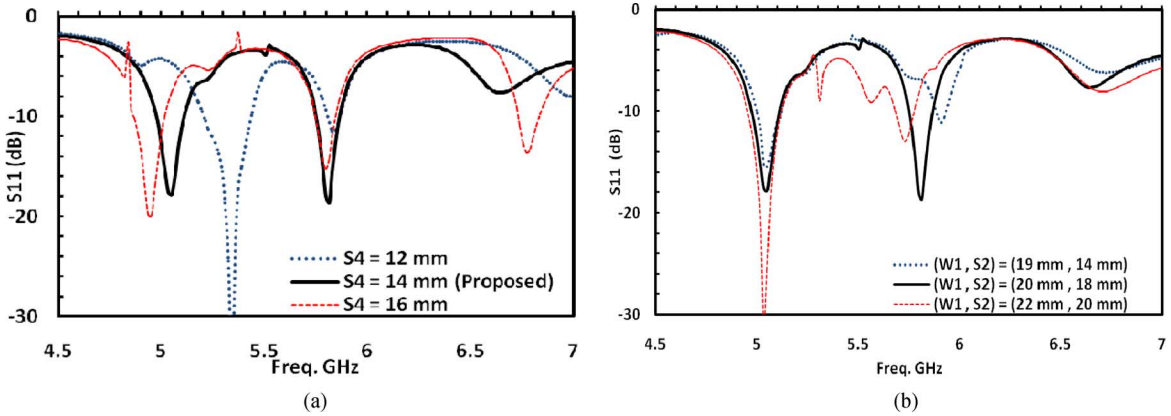


Fig. 8. In ON-OFF state: (a) effects of  $S_4$  on lower band of dual band and (b) effects of  $W_1$  and  $S_2$  together on higher band of dual band.

TABLE III  
MEASURED PEAK GAINS

Switches status (frequency bands in GHz)	ON-OFF (5 & 5.7)	OFF-ON (5.6 & 6.2)	ON-ON (5 & 7)
Gain in dBi	3.7 and 3.54	3.6 & 4.2	3.17 & 4.92

the patch elements. Simulation results have also shown that the wideband performance in the ON-ON state is not affected when these narrow bands are moved to other frequencies. This degree of freedom further enhances the antenna capability. More simu-

lation tests have shown that the maximum frequency separations that can be achieved between the dual-band in the ON-OFF and OFF-ON states are 130 MHz (5.45–5.58 GHz) and 150 MHz (5.94–6.09 GHz), respectively.

Based on the above discussions, we propose the following simple guidelines to design an antenna for dual-band operation at desirable frequencies:

- 1) Optimize the dimensions of the main radiator (the patches without C-Slots) to operate in the 5.6 GHz band.
- 2) Set the dimensions and positions of the C-Slots in conjunction with the discussion provided in Section III-C.

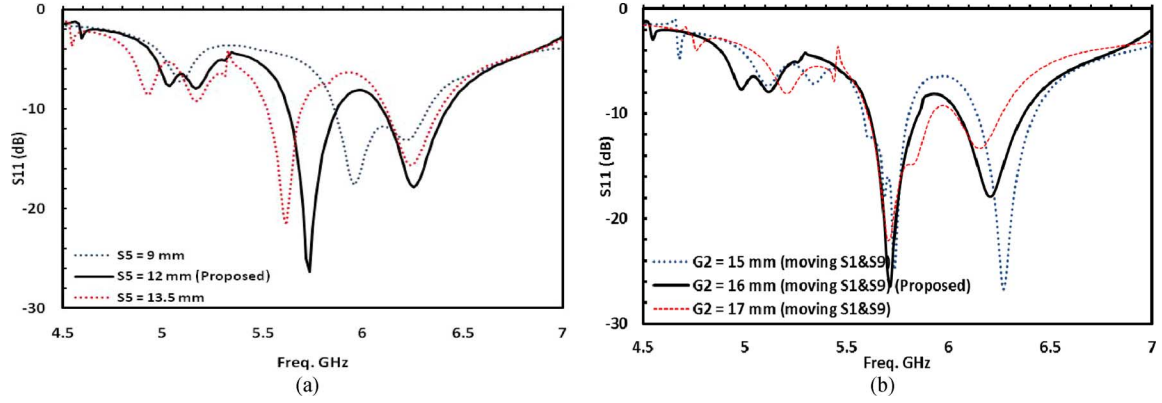


Fig. 9. In OFF-ON state, (a) effects of  $S_5$  on lower band of dual band and (b) effects of  $G_2$  on higher band of dual band.

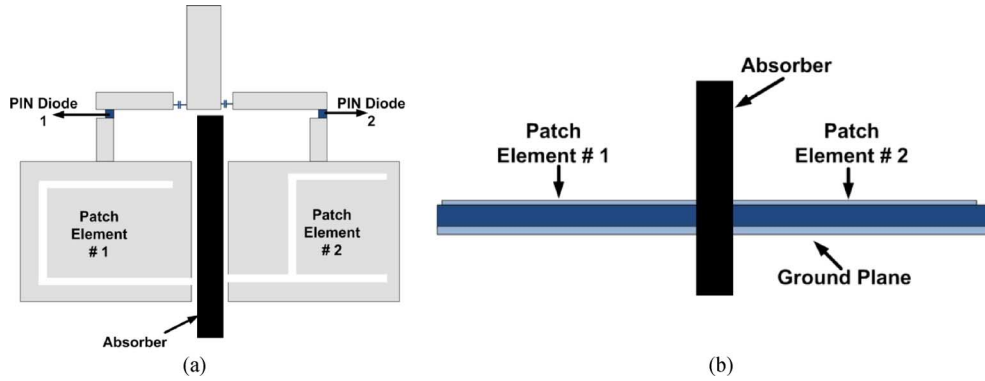


Fig. 10. Antenna with absorber to remove coupling effects (a) Top view and (b) side view.

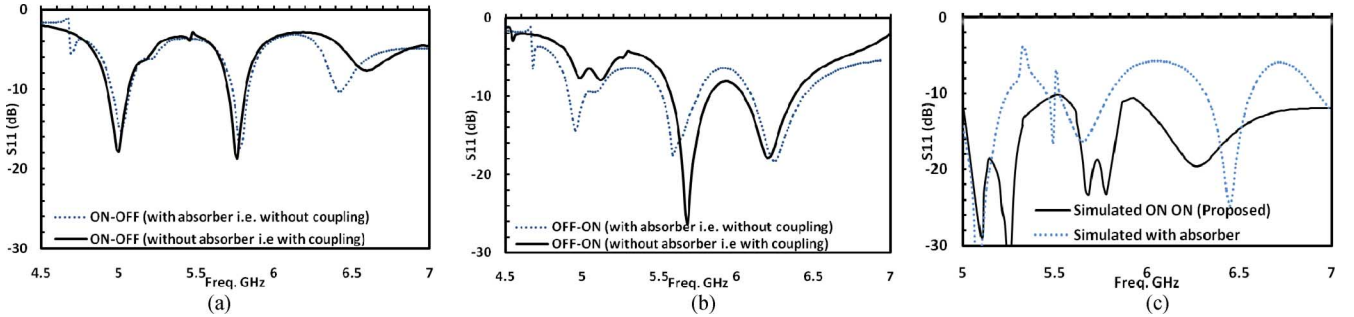


Fig. 11. Reflection coefficient ( $S_{11}$ ) with absorber in (a) ON-OFF (b) OFF-ON, and (c) ON-ON states.

- 3) Adjust the locations and dimensions of the C-Slots on each patch elements to achieve the desirable dual bands. Since they can be independently controlled, this can be easily achieved.
- 4) Optimize the dimensions of the feed network to the patch elements, which is essential for wideband operation.
- 5) Attach the switches and coupling capacitors at the locations given in Fig. 1.

## V. EFFECTS OF COUPLING

Previous results have shown that when both patch elements are ON, the antenna has a wide bandwidth. This must be the results of mutual coupling between the patch elements, which is examined here. To study the coupling effects between the 2 patch elements, we place an EM wave absorber (high lost material) between the 2 patch elements in the simulation model as shown in Fig. 10(a)–(b) to remove the coupling effects and

simulate the impedance bandwidth using  $S_{11}$  in the ON-OFF, OFF-ON and ON-ON states.

With patch element #1 turned ON, patch element #2 turned OFF, and the coupling effect from element #2 to element #1 minimized by the absorber, the simulated  $S_{11}$  is shown in Fig. 11(a). For comparison, the simulated  $S_{11}$  without the absorber, i.e., with coupling, is also shown in the same figure. It can be seen that the differences in  $S_{11}$ , particularly near the dual frequency bands, are quite insignificant, indicating that the coupling between the two patch elements is very small for this case. With patch element #1 turned OFF and patch element #2 turned ON, the simulated  $S_{11}$  with and without the absorber are shown in Fig. 11(b). The differences in  $S_{11}$  near the dual-frequency bands are slightly noticeable. Nevertheless, it is insignificant and so the coupling between the two patch elements is still very small. With both patch elements #1 and #2 are ON, i.e., in the ON-ON state, the simulated  $S_{11}$  with and without the absorber are shown in Fig. 11(c). It can be seen that the mutual coupling between



the 2 elements is much stronger and significantly reduces the  $S_{11}$  to less than  $-10$  dB across the whole frequency band. As a result, the operation bandwidth of the antenna is much wider.

## VI. CONCLUSION

A reconfigurable multiband and wideband patch antenna, employing dual-patch elements and C-Slots with a compact volume of  $50 \times 50 \times 1.57 \text{ mm}^3$ , has been presented and studied using simulation and measurement. Two PIN diode switches are used to switch ON and OFF two patch elements to operate the antenna in two different dual-band modes or a wideband mode (with a bandwidth of 33.52%). The frequencies in the dual-band modes can be independently control using the C-Slots without affecting the wideband performance. Simulation results have shown that the wideband performance is achieved by the coupling effects between the patch elements. The measured and simulated results have shown that radiation patterns across 5–7 GHz are stable in different modes. The main advantages of the proposed antenna include low profile, lightweight and easy to fabricate simple structure targeting future smaller wireless communication devices.

## ACKNOWLEDGMENT

The authors would like to thank Skyworks Solutions, Inc., for providing samples used in this work.

## REFERENCES

- [1] G. Kumar and K. P. Ray, *Broadband Microstrip Antennas*. Boston, MA: Artech House, 2003, pp. 18–23.
- [2] D. M. Pozar and D. H. Schaubert, *Microstrip Antennas*. New York: IEEE Press, 1995.
- [3] H. Wang, X. B. Huang, and D. G. Fang, "A single layer wideband U-slot microstrip patch antenna array," *IEEE Antennas Wireless Propag. Lett.*, vol. 7, pp. 9–12, 2008.
- [4] C. Mak, R. Chair, K. Lee, K. Luk, and A. Kishk, "Half U-slot patch antenna with shorting wall," *Elect. Lett.*, vol. 39, pp. 1779–1780, 2003.
- [5] Y. Li, R. Chair, K. M. Luk, and K. F. Lee, "Broadband triangular patch antenna with a folded shorting wall," *IEEE Antennas Wireless Propag. Lett.*, vol. 3, no. 1, pp. 189–192, Dec. 2004.
- [6] S. Qu and Q. Xue, "A Y-shaped stub proximity coupled V-slot microstrip patch antenna," *IEEE Antennas Wireless Propag. Lett.*, vol. 6, pp. 40–42, 2007.
- [7] Y. Lee and J. Sun, "A new printed antenna for multiband wireless applications," *IEEE Antennas Wireless Propag. Lett.*, vol. 8, pp. 402–405, 2009.
- [8] J. Anguera, C. Puente, C. Borja, and J. Soler, "Dual-frequency broadband-stacked microstrip antenna using a reactive loading and a fractal-shaped radiating edge," *IEEE Antennas Wireless Propag. Lett.*, vol. 6, pp. 309–312, 2007.
- [9] K.-L. Wong and W.-H. Hsu, "A broad-band rectangular patch antenna with a pair of wide slits," *IEEE Trans. Antennas Propag.*, vol. 49, no. 9, pp. 1345–1347, Sep. 2001.
- [10] F. Yang, X. Zhang, X. Ye, and Y. Rahmat-Samii, "Wide-band E-shaped patch antennas for wireless communications," *IEEE Trans. Antennas Propag.*, vol. 49, no. 7, pp. 1094–1100, Jul. 2001.
- [11] R. Bhalla and L. Shafai, "Broadband patch antenna with a circular arc shaped slot," in *Proc. IEEE Antennas Propag. Soc. Int. Symp.*, 2002, vol. 1, pp. 394–397.
- [12] A. Sheta and S. Mahmoud, "A widely tunable compact patch antenna," *IEEE Antennas Wireless Propag. Lett.*, vol. 7, pp. 40–42, 2008.
- [13] A. Mak, C. Rowell, R. Murch, and C. Mak, "Reconfigurable multiband antenna designs for wireless communication devices," *IEEE Trans. Antennas Propag.*, vol. 55, no. 7, pp. 1919–1928, Jul. 2007.
- [14] S. Yang, C. Zhang, H. Pan, A. Fathy, and V. Nair, "Frequency-reconfigurable antennas for multiradio wireless platforms," *IEEE Microw. Mag.*, vol. 10, no. 1, pp. 66–83, Feb. 2009.
- [15] Y. Huang and K. Boyle, *Antennas: From Theory to Practice*. Hoboken, NJ: Wiley, 2008, ch. 8.
- [16] E. Ebrahimi and P. S. Hall, "A dual port wide-narrowband antenna for cognitive radio," in *Proc. 3rd Eur. Conf. Antennas Propag. (EuCAP)*, 2009, pp. 809–812.
- [17] F. Ghanem, P. S. Hall, and J. R. Kelly, "Two port frequency reconfigurable antenna for cognitive radios," *Elect. Lett.*, vol. 45, pp. 534–536, 2009.
- [18] R. Kelly, P. S. Hall, and P. Gardner, "Integrated wide-narrow band antenna for switched operation," in *Proc. 3rd Eur. Conf. Antennas Propag.*, 2009, pp. 3757–3760.
- [19] H. F. AbuTarboush, S. Khan, R. Nilavalan, H. S. Al-Raweshidy, and D. Budimir, "Reconfigurable wideband patch antenna for cognitive radio," in *Loughborough Antennas Propag. Conf.*, 2009, pp. 141–144.
- [20] C. A. Balanis, *Antenna Theory*, 2nd ed. New York: Wiley, 1997.
- [21] J. Volakis, *Antenna Engineering Handbook*. New York: McGraw-Hill, 2007.
- [22] R. Sujith, V. Deepu, D. Laila, C. Aanandan, K. Vasudevan, and P. Mohanan, "A compact dual-band modified T-shaped CPW-fed monopole antenna," *Microw. Opt. Technol. Lett.*, vol. 51, no. 4, pp. 937–939, 2009.
- [23] S. Lee, H. Park, S. Hong, and J. Choi, "Design of a multiband antenna using a planner inverted-F structure," in *Proc. 9th Int. Conf. Adv. Commun. Technol.*, 2007, vol. 3, pp. 1665–1668.



**Hattan F. Abutarboush** (M'07) received the B.Sc. (Eng) Honors degree in electrical communications and electronics engineering from Greenwich and MSA University, London, U.K., in 2005, the M.Sc. degree in mobile personal and satellite communications from the Department of Electrical and Electronics Engineering, Westminster University, London, in 2007, and the Ph.D. degree in antennas and propagations from the Department of Electronics and Computer Engineering, Brunel University, West London, U.K., in July 2011. His Ph.D. research work was mainly on fixed and reconfigurable multiband antennas.

He was a Research Visitor at Hong Kong University in December 2010 and worked as a Research Associate for the American University in Cairo (AUC), Cairo, Egypt, from April to July 2011 where he worked on the packaging of novel millimeter-wave antennas. He has published several journal articles and conference papers. He was invited for special session on multiband antennas at ICEAA 2009 (Italy). His current research interests lie in the design of reconfigurable antennas, antennas for mobile phones, miniaturized antennas, multiple antennas, smart antennas, antenna arrays, EBG, RF/microwave circuit design, and millimeter-wave antennas.

Dr. Abutarboush is a member of IET and a reviewer for several journals and international conferences.



**R. Nilavalan** (M'05–SM'10) received the B.Sc. Eng. degree in electrical and electronics engineering from the University of Peradeniya, Peradeniya, Sri Lanka, in 1995 and the Ph.D. degree in radio frequency systems from the University of Bristol, Bristol, U.K., in 2001.

From 1999 to 2005, he was a Researcher at the Centre for Communications Research (CCR), University of Bristol. At Bristol, his research involved theoretical and practical analyses of post-reception synthetic focusing concepts for near-field imaging and research on numerical FDTD techniques. Since 2005, he has been with the electronics and computer engineering subject area, Brunel University, where he is currently a Lecturer in wireless communications. His main research interests include antennas and propagation, microwave circuit designs, numerical electromagnetic modeling, and digital video broadcast techniques. He has published over 70 papers and articles in international conferences and journals in his research area.

Dr. Nilavalan was a member of the European commission, Network of Excellence on Antennas (2002–2005) and a member of the IET.





**S. W. Cheung** (M'82–SM'02) received the B.Sc. degree (First Class Honors) in electrical and electronic engineering from Middlesex University, Middlesex, U.K., in 1982 and the Ph.D. degree from Loughborough University, Loughborough, U.K., in 1986.

From 1982 to 1986, he was a Research Assistant in the Department of Electronic and Electrical Engineering, Loughborough University of Technology, where he collaborated with Rutherford Appleton Laboratory and many U.K. universities to work a project for new generations of satellite systems.

From 1986 to 1988, he was a Post-Doctorate Research Assistant with the Communications Research Group of King's College, London University, working on research for future generations of satellite systems. In 1988, he joined the Radio and Satellite Communications Division in British Telecom Research Laboratories as an Assistant Executive Engineer. He is an Associate Professor at the University of Hong Kong. His current research interests include antenna designs, 2G, 3G, and 4G mobile communications systems, MIMO systems and satellite communications, predistortion of high-power amplifiers and e-learning. He has published over 130 technical papers in international journals and conferences. He also has served as reviewer for different international journals and conferences in the areas of antennas and propagation and mobile communications.

Dr. Cheung has been serving the IEEE in Hong Kong for the past 20 years. In 2009 and 2010, he was the Chairman of the IEEE Hong Kong Joint Chapter on Circuits and Systems and Communications. Currently, he is the Treasurer of the IEEE Hong Kong Section.

**Karim M. Nasr** (M'05–SM'11) received the Ph.D. degree in smart antenna systems for indoor wireless networks from the University of Manchester, Manchester, U.K., in 2005.

He previously held postdoctoral research positions at the University of Manchester, Brunel University, and BBC Research investigating future wireless and broadcast communication systems through a number of U.K. and European research projects. He was also a Visiting Researcher at the Antennas and Propagation Division of Aalborg University. He is currently a Higher Research Scientist at the National Physical Laboratory (NPL), Teddington, U.K., investigating advanced wireless communication systems and high-precision large-volume laser-based metrology. His research interests include propagation measurements and modeling, DSP and metrology for broadband wireless and broadcast systems, smart antennas and multiuser MIMO systems, UWB, joint Physical/MAC layers optimization and coexistence of wireless systems, advanced antenna metrology, and laser-based coordinate metrology.

Dr. Nasr is a reviewer for several IEEE Transactions and a member of TPC of several wireless international conferences. He is a senior member of the IET and European COST Actions 273 and 2100 on wireless communication systems.



**Thomas Peter** received the M.Eng. degree in electrical engineering from the University Technology Malaysia (UTM), Johor Bahru, Malaysia, in 2007. He is currently pursuing the Ph.D. degree in electronics and computer engineering at Brunel University, West London, U.K.

His current research interest includes UWB antennas and communications, transparent antennas for green technology, energy harvesting and low detection antennas for stealth. From January to March 2011, he was a Visiting Researcher at the

University of Hong Kong to develop transparent green antennas for UWB applications as part of a collaborative research effort. He is currently involved also on collaborative research works with Queen Mary University of London and University of Cambridge.

Mr. Thomas was awarded a VC's travel prize by the Graduate School of Brunel University in November 2010 to present his research paper on the development of a Green UWB antenna at the ISAP2010 conference in Macau.



**Djurdadj Budimir** (M'93–SM'02) received the Dipl. Ing. and M.Sc. degrees in electronic engineering from the University of Belgrade, Belgrade, Serbia, and the Ph.D. degree in electronic and electrical engineering from the University of Leeds, Leeds, U.K.

In March 1994, he joined the Department of Electronic and Electrical Engineering, Kings College London, University of London. Since January 1997, he has been with the School of Electronics and Computer Science, University of Westminster, London, U.K., where he is now a Reader of wireless communications and leads the Wireless Communications Research Group. He has authored and coauthored over 240 journal and conference papers in the field of RF, microwave and millimeter-wave systems. He is the author of the books *Generalized Filter Design by Computer Optimization* (Artech House, 1998) and *Software and Users Manual EPFIL-Waveguide E-plane Filter Design* (Artech House, 2000), and a chapter in the book *Encyclopaedia of RF and Microwave Engineering* (Wiley, 2005). His research interests include analysis and design of hybrid and MMIC, design of amplifiers, filters and multiplexing networks for RF, microwave and millimeter-wave applications and RF, and microwave wireless system design.

Dr. Budimir is a Member of the EPSRC Peer Review College and a Charter Engineer.



**Hamed Al-Raweshidy** (M'92–SM'97) received the Ph.D. degree from Strathclyde University, Glasgow, U.K., in 1991.

He was with Space and Astronomy Research Centre (Iraq), PerkinElmer (USA), Carl Zeiss (Germany), British Telecom (Oxford), Manchester Met., and Kent University. He is currently the Director of the Wireless Networks and Communications Centre (WNCC), Brunel University, London, U.K. He published over 250 papers in international journals and referred conferences. He is the editor of the first book in Radio over Fibre Technologies for Mobile Communications Networks and contributed chapters for six books. He is Editor-in-Chief of *Communication Networks Journal* (USA). He has acted as Guest Editor for the *International Journal of Wireless Personal Communications*. He is a member of several journal editorial boards such as the *Journal of Communications and Mobile Computing* and *Journal of Wireless Personal Communications*. He act as a consultant and involved in projects with several companies and operators such as Vodafone (U.K.), Ericsson (Sweden), Andrew (USA), NEC (Japan), Nokia (Finland), Siemens (Germany), Franc Telecom (France), Thales (U.K. and France), and Tekmar (Italy). He has been able to attract over £3,000,000 from research projects.